SAE TECHNICAL PAPER SERIES

2004-01-1477

Fuel Cell APU for Silent Watch and Mild Electrification of a Medium Tactical Truck

Zoran Filipi, Loucas Louca, Anna Stefanopoulou, Jay Pukrushpan, Burit Kittirungsi and Huei Peng
Automotive Research Center
University of Michigan

Reprinted From: Fuel Cell Power for Transportation 2004 (SP-1827)

ISBN 0 7680 1423-9
9 780768 014235

SAE International™

**2004 SAE World Congress
Detroit, Michigan
March 8-11, 2004**

All rights reserved. No part of this publication may be reproduced, stored in a retrieval system, or transmitted, in any form or by any means, electronic, mechanical, photocopying, recording, or otherwise, without the prior written permission of SAE.

For permission and licensing requests contact:

SAE Permissions
400 Commonwealth Drive
Warrendale, PA 15096-0001-USA
Email: permissions@sae.org
Fax: 724-772-4891
Tel: 724-772-4028

For multiple print copies contact:

SAE Customer Service
Tel: 877-606-7323 (inside USA and Canada)
Tel: 724-776-4970 (outside USA)
Fax: 724-776-1615
Email: CustomerService@sae.org

ISBN 0-7680-1319-4
Copyright © 2004 SAE International

Positions and opinions advanced in this paper are those of the author(s) and not necessarily those of SAE. The author is solely responsible for the content of the paper. A process is available by which discussions will be printed with the paper if it is published in SAE Transactions.

Persons wishing to submit papers to be considered for presentation or publication by SAE should send the manuscript or a 300 word abstract of a proposed manuscript to: Secretary, Engineering Meetings Board, SAE.

Printed in USA

2004-01-1477

Fuel Cell APU for Silent Watch and Mild Electrification of a Medium Tactical Truck

Zoran Filipi, Loucas Louca, Anna Stefanopoulou, Jay Pukrushpan, Burit Kittirungsi and Huei Peng
Automotive Research Center
University of Michigan

Copyright © 2004 SAE International

ABSTRACT

This paper investigates the opportunities for improving truck fuel economy through the use of a Fuel Cell Auxiliary Power Unit (FC APU) for silent watch, as well as for powering electrified engine accessories during driving. The particular vehicle selected as the platform for this study is a prototype of the Family of Medium Tactical Vehicles (FMTV) capable of carrying a 5 ton payload. Peak stand-by power requirements for on-board power are determined from the projected future digitized battlefield vehicle requirements. Strategic selection of electrified engine accessories enables engine shutdowns when the vehicle is stopped, thus providing additional fuel savings. Proton Exchange Membrane (PEM) fuel cell is integrated with a partial oxidation reformer in order to allow the use of the same fuel (JP8) as for the propulsion diesel engine. The APU system is modeled and linked with the complete vehicle system simulation, and accessory duty cycles are derived for both silent watch and driving. The results indicate six-fold improvements of the silent watch fuel economy with the FC APU compared to main-engine idling, and relatively modest improvements from the mild electrification and FC APU use during the driving cycle. Combined fuel economy benefits calculated over the hypothetical daily military mission with a combined 10 hour highway/local/off-road driving and 10 hour silent watch are 20.1%.

INTRODUCTION

Current truck related research initiatives such as the 21st Century Truck, DOE's Program on Reduction in Parasitic Energy Losses for Class 3-8 Trucks, Future Tactical Trucks Systems and Future Combat Systems call for significantly improved fuel efficiency, while preserving or improving truck mobility and freight carrying capacity. Total fuel consumption of commercial trucks in U.S. is more than 42 billion gallons per year, and in recent years it has been steadily growing. The strong impact of the price of fuel on economy and operational cost of freight fleets stimulates development of fuel efficient technologies. In military applications, the impact of the fuel economy is amplified, due to the fact that much of the present logistics support is devoted to moving fuel. The Army transformation requires ability to operate with an agile, more deployable force and a smaller logistics tail. This translates into a technical goal of improving the fuel economy. Given the complex mission of military trucks, the fuel economy needs to be considered not only during driving, but also for silent watch, i.e. when the truck is parked and the crew performs surveillance or communication tasks. Similarly, about one million heavy duty line haulers have sleeper cabins that require energy for ventilation, climate control and various accessories while the driver is resting. Hence, fuel economy, as well as noise and gaseous emissions generated while providing power for cabin auxiliary (hotel) loads during stops are receiving increasingly more attention in the commercial sector.

The effectiveness of some of the approaches for increasing vehicle fuel economy, previously developed for passenger cars, is limited when applied to heavier vehicles. Specifically, opportunities for truck mass reduction are limited due to structural constraints, as well as the fact that reduction of truck's weight is typically viewed as one of the avenues for possible increases in payload rating. In addition, medium and heavy trucks are normally equipped with highly-efficient diesel engines. Consequently, advanced hybrid propulsion systems and reduction of parasitic losses are identified as critical enablers on the technology roadmap to future ultra-efficient truck systems. Electrification of accessories and use of an Auxiliary Power Unit is seen as being particularly effective in reducing parasitics and fuel consumption associated with hotel loads. While fuel cells are considered not to be ready for heavy propulsion, the technology has already been demonstrated on a smaller scale suitable for APU [1, 6].

Both military and commercial sectors are keenly interested in APUs providing stand-by electric power for on-board devices. Examples of these advanced technology devices in military trucks include advanced radio communication equipment, navigation systems, GPS, movement tracking systems, night vision systems,

cabin ventilation, Air Conditioning (A/C) and Nuclear Biological and Chemical (NBC) protection systems, computers, and displays. The US Army projects the need for up to 10 kW of electric power for various battlefield equipment per Dobbs et al. [1], while maintaining minimal thermal and acoustic signature. Power for these devices needs to be available during driving as well as when the vehicle is parked, i.e. during a silent watch. Traditionally, the silent watch for military trucks is provided by propulsion engine idling and running the alternator. This forces the engine to operate at a very inefficient regime for extended periods of time, and creates undesirable noise and gaseous emissions. The option of a small ICE or gas turbine APUs allows much more efficient operation, but noise and thermal signature still require very careful management. Hence, the Fuel Cell APU is a very attractive alternative, offering a well rounded trade-off among fuel economy, energy density and low thermal/acoustic signature.

The focus of this work is the feasibility analysis and evaluation of fuel economy benefits of using the Fuel Cell APU to power the electrified engine and vehicle accessories. The particular vehicle selected as the platform for this study is the prototype version of the Family of Medium Tactical Vehicles (FMTV) with a 6x6 drivetrain, capable of carrying a 5 ton payload over a smooth or rough terrain. Fuel economy potential of hybridization of Class VI trucks was addressed in previous simulation studies – see [2, 3, 4]. In particular, work published by Filipi et al. [4], addressed the selection of the hybrid architecture, presented modeling of the complete vehicle system, and proposed the methodology for sequential optimization of hybrid propulsion system design and power management. The results demonstrated the effectiveness of the hydraulic hybrid (HH) propulsion system in regenerating and reusing the braking energy. Hence, the HH FMTV prototype vehicle is the starting point for the study of the additional benefits provided by the APU. Very high number of FMTVs in army fleets implies high impact of possible future insertion of new technologies into the medium tactical trucks.

The option of using a FC APU has recently attracted a lot of attention and initial studies have shown the viability of 5 kW units for cabin auxiliaries [6, 7, 8, 9]. In parallel, researchers considered opportunities for reducing engine parasitic losses (parasitics) by using controllable, electric engine accessories, e.g. Hnatzuk et al. [10] evaluated the potential for savings through electrification of coolant and water pumps, while Hendricks et al. [11] performed a comprehensive study of the benefits of removing belt-driven mechanical loads, but without addressing the impact of replacing the mechanical loads with electric loads. The work presented here introduces a combined approach, i.e. in addition to using the FC APU for supporting the silent watch requirements, we propose to electrify some of the engine accessories and use the FC APU to power them during driving. This enables accessory control for reduced power consumption and efficient power generation, thus contributing to improved driving fuel economy. The concept is illustrated in Figure 1. Strategic selection of electrified accessories enables engine shut-down when the vehicle is stopped, thus providing additional fuel savings. The Fuel cell APU system consists of a JP8 Fuel Processor (FP) system, and a Proton Exchange Membrane (PEM) Fuel Cell (FC) system that includes the air delivery, humidification and cooling sub-systems. The reformer of the FP system is assumed to be based on a catalytic partial oxidation process [12]. The PEMFC is sized based on the estimated combined silent watch and engine electrification requirements. The original FMTV battery pack (four 14V 6MTF Lead-Acid batteries) is used to supplement the FC APU power output during fast changes in load demand.

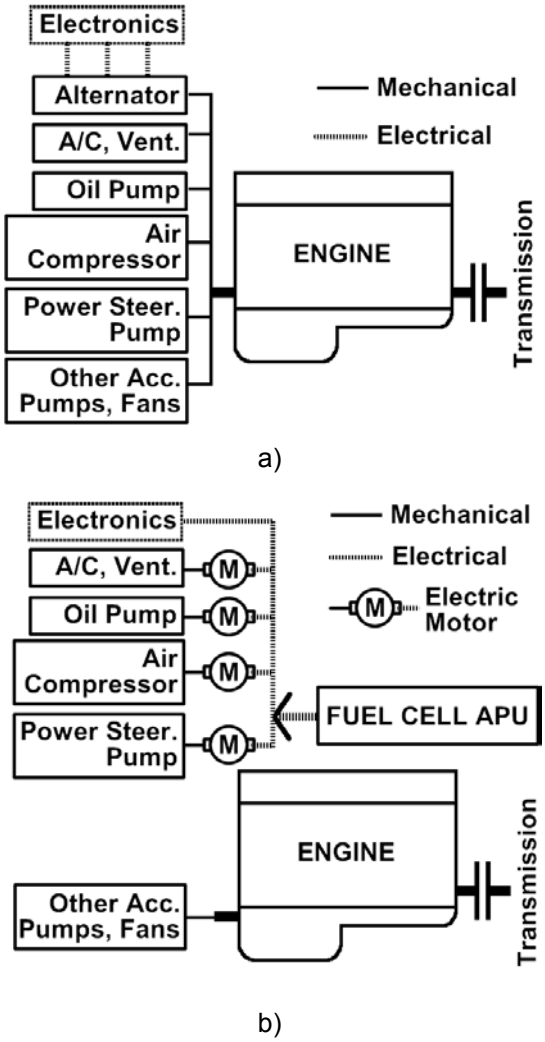

Figure 1: Schematic of the engine with accessories: a) original configuration and b) proposed accessory electrification and the use of FC APU

The study first surveys the electric and electronic loads from typical cabin devices and equipment aboard the tactical vehicle. Then, we identify a set of accessories that hold a promise of tangible energy savings if decoupled from the engine crankshaft and electrified. Selecting engine oil pump, power steering pump and air brake compressor allows shut-downs of the engine during vehicle stops. Next, modeling and integration of the complete vehicle system is presented, followed by

the details of FC APU modeling and control. Silent watch mission profile that captures auxiliary power requirements during a ten hour period is constructed. Duty cycles for engine/drivetrain accessories are devised based on their function and in conjunction with the actions taken during the driving schedule. Then, a sequence of simulations is performed for the silent watch and the vehicle following the representative driving schedule. Finally, conclusions about the fuel economy potential of the proposed concept are given in the last section.

STAND-BY POWER REQUIREMENTS

Auxiliary power requirements on modern trucks are rapidly increasing due to growing demand for electronic equipment, driver protection and comfort. The projections for future military trucks are based on the plans for army transformation and battlefield digitization. Equipment necessary for digitization of the tactical vehicle includes digital radio systems, navigation systems (GPS, 3D mapping), encryption systems, computer and displays, movement tracking system (MTS), identification friend-or-foe, and driver vision enhancement (DVE) [1]. In addition, Nuclear, Biological and Chemical (NBC) protection requires high-capacity ventilation system for over pressurizing the cabin combined with air/conditioning. Power for this equipment needs to be available at any time, during driving as well as during extended stand-by periods. The stand-by requirements should be preferably met with minimal noise and thermal emission, hence the term silent watch.

For tactical trucks, such as the FMTV, the estimated peak power requirement for the ventilation, NBC protection and air-conditioning is 3.4 kW. The communication equipment's maximum power consumption is 0.6 kW. It is estimated that the rest of the electronics, such as navigation, MTS, DVE, displays etc., will require another 0.6 kW. This brings the total peak auxiliary power requirement to 4.6 kW. Duty cycles for electronics and other auxiliaries are discussed in the dedicated section given in the latter part of the paper.

There are generally three ways of providing power for auxiliaries during stand-by: discharging batteries, engine idling and running the alternator, and using an Auxiliary Power Unit. The APU can be based on a generator-set powered by a small IC engine, micro-turbine, or a fuel cell.

Batteries found on the FMTV truck (four military batteries) exceed the average size, due to cold start requirements. Nevertheless, their ability to sustain stand-by loads for extended period of time is very limited. The main determining factors are the state-of-charge lower limit that guarantees safe restarting of the engine, and the effect of the depth of recycling on battery life. Dobbs [1] estimates the practical stand-by operation, using only electronics (no A/C), to be up to 30 minutes with two military batteries. This would increase to one hour on the FMTV equipped with four batteries – still far less than the expected length of the silent watch of 4 – 10 hours. Hence, on most military vehicles engine idling is used as the source of energy for extended stand-by. Unfortunately, while heavy-duty diesels provide very good efficiency at high loads, their fuel economy is much poorer at idling. Extended idling in cold weather often leads to deteriorated diesel combustion and over-fueling, which can lead to diluting of oil and increased wear. In addition, engine noise emission can not provide the truly silent operation, and its exhaust emission provides unwanted heat signature.

Using an APU with a small IC Engine can dramatically improve the stand-by fuel consumption, but is still accompanied by the noise and thermal signature. The micro-turbine APU is typically less economical and more costly than the ICE APU. This makes the Fuel Cell APU worth exploring.

While this paper focuses on a typical tactical truck, it is worth noting that the total power requirement for the commercial Class 8 vehicle with a sleeper cabin would be very similar. The ventilation and A/C system are comparable, and cabin comfort and entertainment features, e.g. electric coffee maker, refrigerator, hair-dryer, TV and video equipment, replace the extensive use of battlefield electronics. Consequently, total stand-by requirement for a commercial truck is approximately 5 kW [6, 7, 9]. It is estimated that roughly half a million trucks idle between 3.3 and 16.5 hours a day, and 18 states already have anti-idling regulations. Using a Fuel Cell APU would offer similar benefits as in the military application. In addition, availability of the Fuel Cell APUs on dual-use vehicles would enable on-site generation and increase mission flexibility in case of disaster and relief efforts.

ELECTRIFICATION OF ACCESSORIES

The engine/drivetrain accessories enable functioning of the systems critical for safe engine and vehicle operation, such as cooling, lubrication, steering and braking. In the conventional engine/drivetrain configuration all of the main accessories are mechanically driven by the engine. The direct mechanical coupling makes accessory speed dependant on engine speed and severely limits our ability to control its operating conditions. Electrification offers potential fuel savings through accurate control of accessories independent of instantaneous engine speed.

The concept is illustrated using the power steering pump as an example. When the steering wheel is turned, the power steering system provides assist using the pressurized fluid supplied by the pump. The pump is sized so that it can satisfy the required fluid pressure and flow even at low engine speeds. This determines the nominal torque needed to drive the pump. However, as the engine speeds up, the relief valve opens in order to limit the pressure, the torque remains roughly constant, but the consumed power increases almost linearly with speed – see Figure 2. In addition, even when the pump is unloaded, internal friction losses will

cause small, but non-negligible power consumption. If the pump is decoupled from the engine, it can be operated only when needed and always at the most efficient point. In case of the FMTV vehicle, this reduces the peak power requirement from 12.9 kW to only 4.2 kW, as shown in Figure 2. In addition, the power consumption is reduced from 0.7 kW to zero when there is no steering. Similar reasoning regarding the nominal power consumption can be applied to the engine oil pump, as shown by Hnatczuk et al. [10].

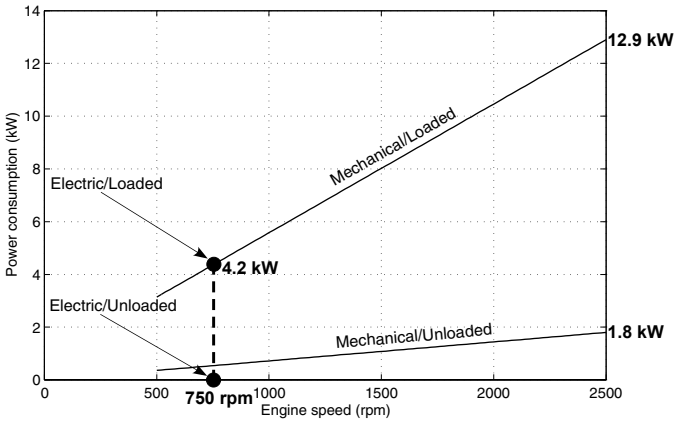

Figure 2: Power consumption of the mechanically driven power steering pump and the desired operating point achievable with the electrified version

The accessories of the FMTV vehicle that are considered in the analysis and their peak power requirements are as follows: engine fan 26 kW, transmission fluid pump 15 kW, power steering pump 12.9 kW, air brake system compressor 3.7 kW, engine oil pump 4 kW, and engine cooling pump 2 kW. The biggest consumers, e.g. engine fan, are too large for a practical FC APU design. Prime candidates for electrification were selected considering the ease of implementation and savings that can be provided by allowing engine shut-downs when the vehicle is stopped. Thus, the engine oil pump, power steering pump and air compressor are electrified in the virtual vehicle equipped with the FC APU.

The peak power requirement for the original, mechanically driven components is 4+12.9+3.7 = 20.6 kW. However, electrifying the same three components reduces the peak requirement to 1.4+4.2+1.2 = 6.8 kW for the reasons explained earlier in this section and depicted in Figure 2. The APU needs to fulfill this requirement during driving, in addition to the power needed for cabin auxiliaries described in the previous section. Consequently, the total peak power requirement is 11.4 kW. In reality, it is unlikely that all of the accessories will operate at their peak at any given instant in time, and even if this occurs the battery on the vehicle is fully capable of acting as a buffer and covering the short term deficit. Thus, the practical sizing target for the FC APU is set at 10 kW.

VEHICLE DESCRIPTION AND MODELING

The vehicle system is based on the 5-ton standard cargo vehicle from the Family of Medium Tactical Vehicles with a gross vehicle weight of 15,300 kg. It's a 6X6, full time all wheel drive truck, powered by a 246 kW six-cylinder, turbocharged, intercooled, direct injection diesel engine coupled to a 7-speed automatic transmission. For the modeling purposes of this study, the FMTV truck is decomposed into the engine, drivetrain, hydraulics and vehicle dynamics. The schematic of the propulsion of this hybrid vehicle is shown in Figure 3. Since the emphasis of the work is fuel economy the torque look-up table based engine model is used, rather than a high-fidelity thermodynamic model previously used for studies of engine transient response [21]. In the conventional drivetrain, diesel engine drives the vehicle through the torque converter (TC), whose output shaft is then coupled to the automatic transmission (AT), which drives the transfer case (TrC) that equally splits the torque to the front and rear wheels. The front prop-shaft delivers the torque to the front differential (DF). The other output of the transfer case, through the rear-front prop-shaft, delivers power to the inter-axle transfer case (TrCA) that further splits the torque to the two rear axles. The first output of the inter-axle transfer case drives the rear-front differential (DRF) and the other the rear-rear differential (DRR) through the rear-rear prop-shaft. Finally, the torque is delivered to the wheels through the half-shafts.

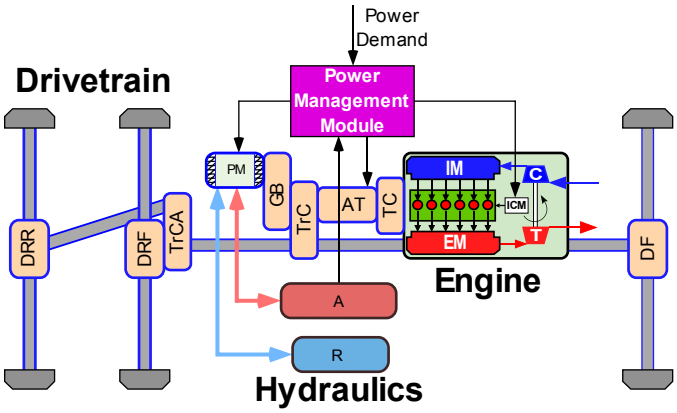

Figure 3: Schematic of the 6x6 truck with the parallel hydraulic hybrid propulsion system

In addition to the conventional components, the drivetrain includes a hydraulic pump/motor (PM), accumulator (A), and reservoir (R) to provide the hybrid functionality. The pump-motor is connected to the transfer case after a fixed speed reduction provided by a gearbox (GB). The pump/motor is connected to the accumulator that stores a high-pressure hydraulic fluid by means of compressed gas. On the other hand, the reservoir stores or supplies the hydraulic fluid used by the pump/motor. The operation of the hybrid drivetrain is controlled by the power management module that determines the operating points of the engine, transmission, and pump/motor based on the power demand and the available hydraulic fluid in the accumulator.

The drivetrain drives the three solid axles of the FMTV truck, which are connected to the chassis with leaf spring suspensions and shock absorbers. Due to the particular focus on fuel economy, the lateral motion of the vehicle is neglected. Therefore, the model assumes left-right symmetry that results in a planar pitch plane model with only three degrees of freedom for the vehicle motion.

The basis for the FMTV component modeling is the previously developed high-fidelity Vehicle-Engine Simulation (VESIM) environment [20, 21, 22]. VESIM has been validated against measurements and proven a very versatile tool for mobility, fuel economy and drivability studies [21]. VESIM emphasizes the high degree of model fidelity and feed-forward logic, thus enabling studies of transient conditions and easy implementation and evaluation of controllers. The model is developed in the 20SIM system modeling and simulation environment that supports hierarchical modeling and allows the physical modeling of subsystems and components using the bond graph formulation [23, 24]. This environment allows easy modification (addition or removal) of model complexity, which makes model development a straightforward task. The model can be easily developed by including only the necessary physical phenomena that contribute to the response of interest, i.e. fuel economy. Model complexity is systematically identified using an energy-based model reduction technique [25].

At the top level of the model hierarchy (see Figure 4), the engine, drivetrain, hydraulics, and vehicle dynamics are excited by the environment. One source of excitation is the driver who controls the vehicle velocity through the gas and brake pedal. The cyber driver is modeled as a controller that attempts to follow the driving cycle. Due to the off-road driving of the truck, the other excitation comes from the road, which is usually uneven and prescribes a vertical velocity to the tires at the contact point. The road excitation is applied to the front, rear-front, and rear-rear tires as a function of their longitudinal position. A more detailed description of the complete FMTV model can be found in [4].

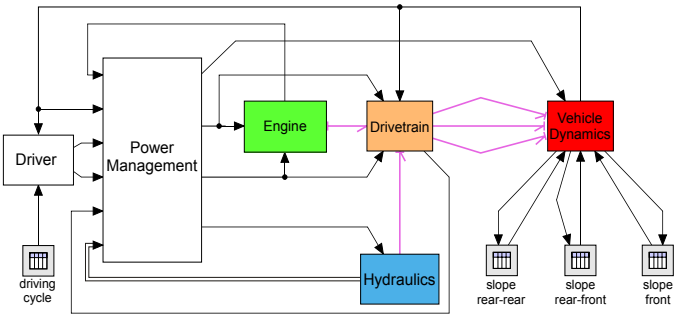

Figure 4: VESIM model of the FMTV truck

ACCESSORIES MODELING

As previously described, engine accessories will be considered for electrification due to the potential reduction of parasitic losses and fuel economy improvements. Alternative design configurations will be considered; therefore, models of the selected accessories (air-brake compressor, oil pump, AC compressor, and power steering pump) are developed in order to calculate the additional fuel consumption. The flexibility of the VESIM environment allows easy integration within the vehicle system simulation.

The complexity of the engine accessory models depends on their interactions with the system and operating conditions. The dynamics of accessories are orders of magnitude faster from the rest of the vehicle system and their inertial effects are much smaller compared to the engine inertia. Therefore, only the steady-state behavior of these devices is necessary in order to capture the dominant power interactions between the engine and accessories. Such a model will accurately predict the engine response and fuel economy.

Under steady state conditions the power steering pump and air conditioning compressor produce a constant torque load that needs to be provided by the engine (see Figure 5). The actual values of this torque depend on the operation of the accessory and they will be defined later in the paper. These accessories have a one-way coupling with the engine and vehicle, in contrast with the alternator and oil pump loads that are coupled with the engine speed. All accessories are driven by the engine via belts or gears that are represented in the model by transformer elements (TF). The accessories are connected to the engine through the crankshaft port that provides the total torque (T_{ACC}) to drive the accessories.

Given the electric power, $P_{electric}$, needed by the electronics and AC fan, the required torque at the shaft of the alternator is calculated based on engine speed and alternator efficiency. This is done in the "Alternator" block in Figure 5 and the alternator torque (T_A) is applied to the engine. The electric accessory loads are defined as power requirements, which will also be defined later. The oil pump torque (T_{OP}) is a function of engine speed and is calculated from a lookup table obtained from experimental data.

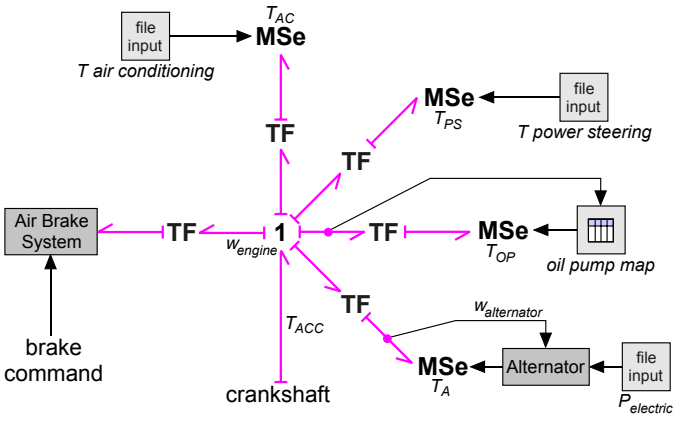

Figure 5: Model of mechanically driven accessories

For the air brake compressor torque, the brake command during driving is used to determine the operation of the compressor. Calculations are performed by the "Air Brake System" block using a dynamic model of the air brake system. This model is depicted in Figure 6. It consists of the compressor and air tanks (wet, primary and secondary). The compressor model provides the airflow (mass and energy) to fill the air tanks based on engine speed and backpressure from air tanks. In addition, it provides the torque load to the engine. This simplified model is derived from a detailed thermodynamic model with complete cycle dynamics and flow through inlet/exhaust valves. The air consumption is calculated based on the brake command where for each brake event an amount of air equivalent to the volume of the six brake chambers is removed from the tanks. The model also includes heat transfer effects between the air tanks and the environment. Finally, a governor is used to maintain the air pressure within the working limits for a safe operation of the brakes. In contrast with the other accessories, there is two-way coupling between the air compressor and engine due to the brake command feedback.

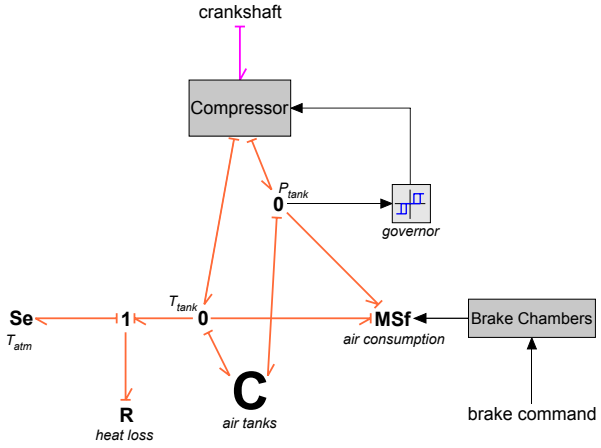

Figure 6: Air-brake system model

For electrically driven accessories the model is modified since the accessories are now decoupled from the engine and are driven by the electric power of the FC APU. Therefore, electric motors are used to convert the electric to mechanical power. Design of accessories is unchanged, but their operating speed is assumed to be equivalent to the engine idle speed, which is the minimum speed at which they can have acceptable performance. The alternator is eliminated since the electric loads are directly provided by the FC APU and their electric power is just added to the other power requirements. This model is given in Figure 7 where the GY element represents the motor, which includes the motor constant and mechanical efficiency. The total power (P_{APU}) that the FC APU must supply to drive these accessories is the sum of power of the electrically driven accessories and direct electric loads ($P_{electric}$) given by:

$$P_{APU} = V_{BUS} \cdot i_{ACC} + P_{electric} \quad (1)$$

where V_{BUS} is the electric bus voltage, i_{ACC} is the total current drawn by the accessories.

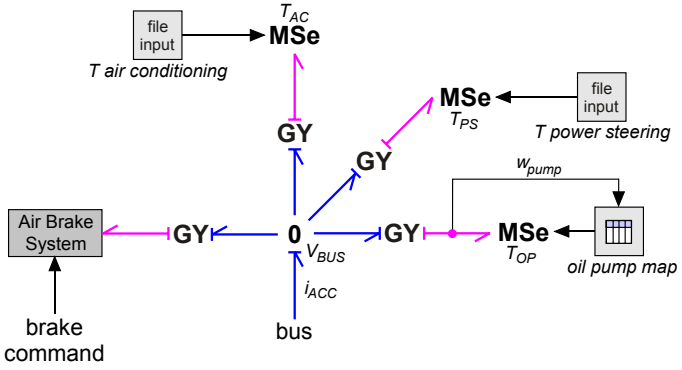

Figure 7: Electrically driven engine accessories

FUEL CELL APU SYSTEM

SELECTION OF COMPONENTS

Among all fuel cell types, the front-runners in APU applications are the Solid Oxide Fuel Cell (SOFC) and Proton Exchange Membrane Fuel Cell (PEMFC). PEMFCs are favored over SOFCs due to their more advanced stage of development, material strength and corrosion characteristics, lower operating temperature, manufacturing process, and relatively lower cost. One of the key issues of PEMFC stacks is that they require hydrogen (H_2) rich gas with almost-zero carbon monoxide (CO) and sulfur concentration. Since storing hydrogen is generally not desired in military applications, a fuel processor (FP) system is adopted to extract hydrogen from the same fuel that is currently used for propulsion, namely JP8. The fuel processor, also known as fuel reformer, is integrated with the PEMFC to form a self-contained FC APU. Venturi et al. demonstrated the use of a FC APU running on methanol [6] and a synthetic fuel that is similar in chemical composition to JP8 [7]. An APU based on fuel processor plus PEMFC is expected to have lower overall efficiency than an APU based on SOFC due to the multiple processes required to develop the H_2 rich gas [14, 19]. We choose to use a PEM Fuel Cell Auxiliary Power Unit with an on-board fuel processor due to their anticipated early adoption in military applications.

A typical fuel processor (FP) consists of four main reactors shown schematically in Figure 8. The liquid fuel is first vaporized and supplied to the first reactor, the hydro-desulfurizer (HDS) for Sulfur removal. The cleaned fuel gas is then supplied to the main reformer, which is responsible for the majority of the H_2 conversion. The gas exiting the main reformer is rich in Hydrogen but contains large quantities of CO_2 and CO. Due to the detrimental effects of CO on the PEMFC, additional reactors are needed to remove CO from the gas stream before it is directed to the fuel cell. Carbon monoxide removal is achieved in three separate reactors: the two water gas shift (WGS) and the preferential oxidation (PROX) reactors.

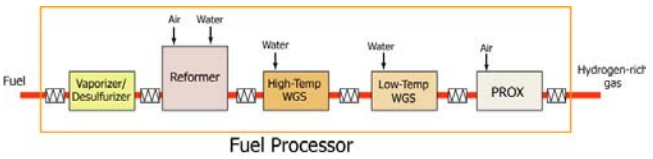

Figure 8: Schematic diagram of a typical Fuel Processor

The two most popular chemical processes to convert hydrocarbon fuel to hydrogen include Steam Reforming (SR) and Partial Oxidation (POX). The most common method, steam reforming, is endothermic, well suited for steady-state operation and delivers relatively high conversion efficiency [16]. However, it suffers from poor transient operation [14]. The partial oxidation process offers several advantages such as compactness, rapid-startup, and responsiveness to load changes [17], but delivers lower efficiency as shown in Table 1.

Table 1: Main H_2 Reactor Efficiency for different Hydrocarbon Fuel and Conversion Principle

Fuel	Energy Efficiency (%)	
	POX	SR
Methanol	Data n/a	83.2
Natural Gas	77.5	85.5
Gasoline	55.8	81.2
Diesel	55.7	81.2
Jet fuel	54.9	81.2

The values of Table 1 are derived from Table 6 in [14] using theoretical input energies for producing a mole of H_2. In particular, the SR and POX efficiencies are calculated from:

$$\eta_{SR} = \frac{Q_{LHV_{H_2}}}{Q_{tTH_{C_xH_y}}} \quad \text{and} \quad \eta_{POX} = \frac{Q_{LHV_{H_2}}}{Q_{TH_{C_xH_y}}} \qquad (2)$$

where:

$Q_{LHV_{H_2}}$ is the H_2 low heating value,

$Q_{tTH_{C_xH_y}}$ is the total theoretical C_xH_y fuel heat input per mole of usable H_2, and

$Q_{TH_{C_xH_y}}$ is the theoretical C_xH_y fuel heat input per mole of usable H_2.

Note here that in the SR case the total Theoretical C_xH_y Fuel Heat input per mole of usable H_2 includes the heat required for the endothermic reaction. The efficiencies in the POX-based fuel processor are calculated without assuming utilization of the exothermic heat. This choice leads to low efficiency assumptions for the POX-based FP system. In all cases, the system efficiency is calculated assuming that the gas leaving the FC anode has 8% hydrogen partial pressure. The molar composition of the fuel affects the Partial Oxidation reactor efficiency. The lowest efficiency (54.9%) is observed when Jet fuel, chemically similar to JP8, is used. Despite of the low efficiency, a POX-based fuel processing system is adopted due to its faster start-up and compact characteristics.

FUEL CELL STACK SIZING AND MODELING

The fuel cell stack (FCS) is sized to satisfy the 10 kW peak power identified in the previous sections. The sizing process has many degrees of freedoms and has to satisfy many constraints. Design degrees of freedom include the number (n) of cells stacked in series, the cell active area (A), the reactant supply pressure, and the cooling method. Typical constraints are the desired vehicle operating voltage, the volume, the weight, and the hydrogen supply method. The PEMFC APU is sized using conservative published data, in order to better evaluate its short term benefits instead of their long-term potential.

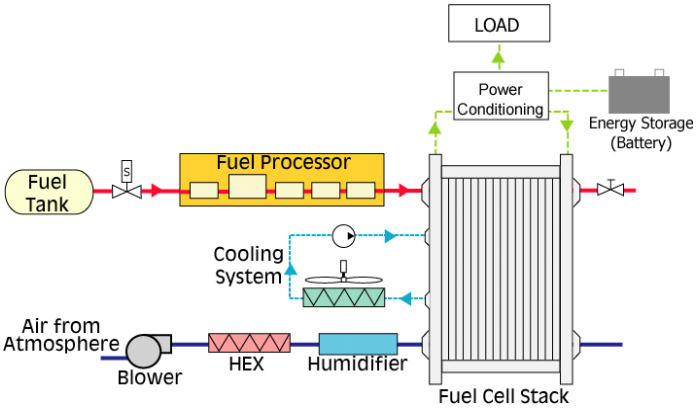

Figure 9: Schematic diagram of the FC APU system

A liquid-cooled low pressure FC system design is selected because it can operate seamlessly with a fuel processing system that typically operates in near-ambient pressure conditions [1]. Its configuration is shown in Figure 9. Non-equilibrium conditions are neglected and a single polarization curve is utilized to describe the electrical output of a single fuel cell. Specifically, Figure 10 shows the single cell voltage (V_{fc}) versus current density ($i=I_{fc}/A$ in A/cm^2) drawn from the fuel cell. The specific characteristic is obtained from [15] under low reactant pressure. We consider only one steady-state polarization curve for all cells within the stack because the current drawn from the fuel cell stack is controlled so that quasi-steady FC conditions are maintained (see FC APU Control section). Due to the electrical connection of *n* cells in series the stack current is equal to the single cell current ($I_{fsc} = I_{fc}$), whereas, the stack voltage is given by ($V_{fsc} = nV_{fc}$).

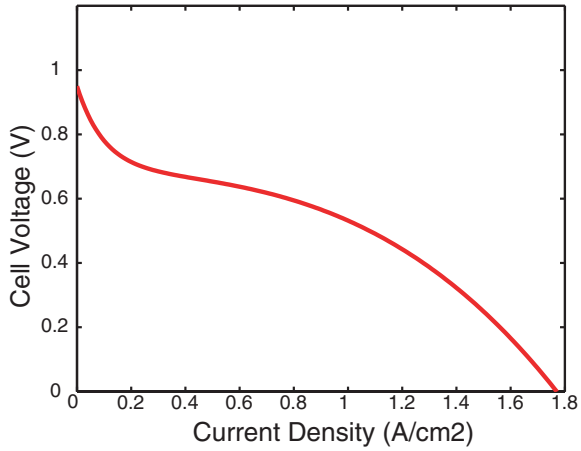

Figure 10: Fuel Cell Polarization Curve

A typical active cell area (250 cm^2 < A < 400 cm^2) and an output stack voltage (V_{fcs} = *42 Volts)* are considered as target values for the FC stack. The parasitic losses (P_{aux}) due to the FCS auxiliary components such as the air blower are captured by a linear function. The minimum auxiliary load is 200 W and it is assumed to increase linearly by 0.57 W/Amp with the load current drawn from the stack. The net fuel cell stack power is then given by:

$$P_{fcs}(I_{fcs}) = nV_{fc}I_{fc} + \max\{0.2, 0.57I_{fc}\} \qquad (3)$$

A simple search procedure shows that n = 65 and A = 300 cm^2 satisfies the system requirements of 42 Volts voltage output and 10 kW power output. The FC stack net power (P_{fcs}) and efficiency values versus the current (I_{fc}) are shown in Figure 11.

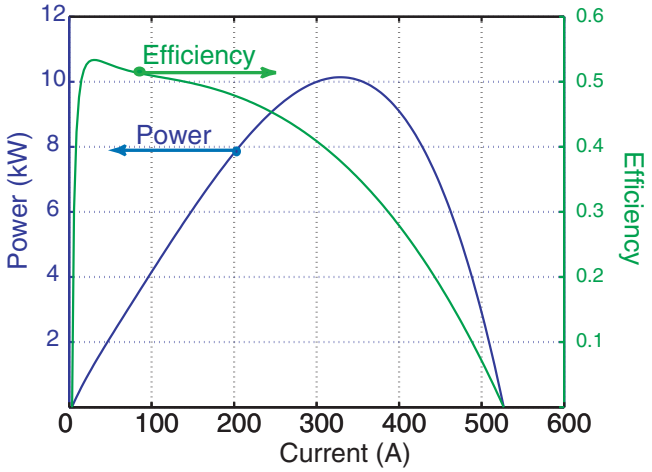

Figure 11: Fuel Cell Stack Power and Efficiency versus Current

The peak FC power $P_{fcs}^{\max}$ = 10.05 kW is attained at stack current I_{fc} = 350 Amps or at the current density value of i = 1.17 A/cm^2. The stack efficiency (η_{fcs}) is defined as:

$$\eta_{fcs} = \frac{P_{fcs}}{nV_0 I_{fc}} \qquad (4)$$

where V_0 is the theoretical maximum single cell voltage also known as the open circuit voltage (from lower heating value).

FUEL PROCESSOR MODELING

The fuel consumption from the Fuel Cell Auxiliary Power Unit is calculated using basic electrochemistry and the conversion efficiency of the fuel processor. Specifically, the hydrogen consumption rate (moles per second) depends on the stack current drawn from the fuel cell system:

$$N_{H_2} = \frac{nI_{fc}}{2F} \qquad (5)$$

where F is the Faraday number (96485 Coulombs). The fuel consumption rate (moles/sec) is then calculated from the POX FP efficiency:

$$N_{fuel} = \frac{Q_{TH_{C_xH_y}}}{Q_{LHV_{C_xH_y}}} N_{H_2} \qquad (6)$$

where $Q_{LHV_{C_xH_y}}$ is the low heating value of the C_xH_y hydrocarbon fuel and $Q_{TH_{C_xH_y}}$ is defined in the previous section. Finally, the mass flow rate (g/s) of the C_xH_y hydrocarbon fuel is calculated from:

$$\dot{m}_{fuel} = M_{C_xH_y} N_{fuel} \qquad (7)$$

where $M_{C_xH_y}$ is the molar mass of the C_xH_y hydrocarbon fuel (in our case JP8). The instantaneous mass flow rate is integrated throughout the driving cycle and the silent watch in order to calculate its impact on the overall fuel consumption.

The dynamic response of the POX-based fuel processor during transient conditions is modeled using a first order lag with a time constant $\tau_{fp} = 1$ sec. This time constant is chosen based on our experience in transient control of a 200 kW natural gas reformer and other published data [12, 18]. Although the system time constant and efficiency actually vary with fuel flow rate (hydrogen flow demand), using a simple first order dynamics with fixed fuel processor efficiency is deemed sufficient for the vehicle system level fuel economy calculations.

FC APU CONTROL

An overview of the FC APU controller that allows integration with the vehicle batteries is shown in Figure 12. The key objectives of the FC APU controller are to:

- Ensure that the requested power is delivered
- Protect the fuel cell stack and fuel processor system from sudden current loads
- Supplement fuel cell system power deficit from batteries without depleting them below a threshold state of charge

The fuel consumption calculations are also included in the model to allow direct implementation within VESIM. The input to the FC APU controller is the desired APU power (P_{APU}). Any power request from the Battery (P_{bt}^{req}) is added to the FC APU power requests to provide the total power demand given by:

$$P_{fcs}^{dem} = P_{apu} + P_{bt}^{req} \tag{8}$$

The overall fuel cell system power demand P_{fcs}^{dem} is then used as the input to a lookup table to calculate the current demand from the FCS (I_{fcs}^{dem}). The lookup table essentially inverts the FCS power function found in Eq.(3) for the stack current calculation.

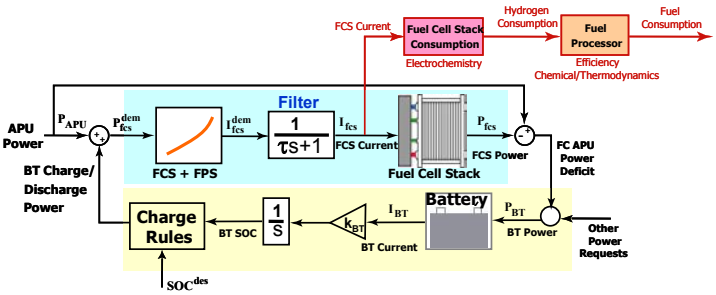

Figure 12: Schematic of the FC APU controller

CURRENT CONTROL AND HYDROGEN STARVATION CONSTRAINTS

The responsiveness of H_2 generation imposes a limitation on how fast stack current can be drawn from the FCS. As discussed before, the FP responds to a step change in hydrogen command with a first order lag in H_2 generation. To avoid H_2 starvation in the FCS anode the current drawn from the fuel cell is always filtered using the FP time constant:

$$I_{fc}(s) = \frac{1}{\tau_{fp}s + 1} I_{fc}^{dem}(s) \tag{9}$$

The current drawn from the FCS is then used to calculate the FCS power P_{fcs} using Eq.(3). The FP time constant thus dominates the fuel cell system dynamics. To support the instantaneous current demands associated with the steering requests or other time-critical functionalities, we employ the existing vehicle battery and integrate it with the FC APU. The deficit between the demanded power from the APU (P_{apu}) and the power delivered by the FCS is supplemented by the vehicle batteries. However, to avoid battery depletion, a separate battery controller is designed which is explained in the next section.

BATTERY STATE OF CHARGE CONTROLLER

The original FMTV battery pack (four 14V 6MTF Lead-Acid batteries) is used to supplement the FC APU power output during pulsed load demand. The power requested and drawn from the battery is:

$$P_{bt} = P_{apu} - P_{fcs} + P_{other} \tag{10}$$

where P_{other} is the additional electrical power demand from the vehicle. A lookup table with the battery efficiency is used to calculate the current drawn from or supplied to the battery during discharging and charging, respectively ($I_{bt} = f_{bt}(P_{bt})$). Note that the power request for the battery is positive when discharging and negative when charging. The battery state of charge (SOC) depends on the battery current (I_{bt}) and the battery rated Amp-Hours ($1/k_{bt}$):

$$SOC(t) = SOC(t_0) - k_{bt}\int_{t_0}^{t} I_{bt}\,d\tau\,. \tag{11}$$

A simple proportional controller defines the power request (P_{bt}^{req}) and consequently regulates the battery state of charge at a desired level (SOC^{des}) selected to be 0.55 :

$$P_{bt}^{req} = k_c\left(SOC^{des} - SOC\right). \tag{12}$$

The controller gain k_c is adjusted based on the desired speed for charging the battery.

MISSION PROFILE/ACCESSORY DUTY CYCLE

Fuel consumption is heavily dependent on the operation of the vehicle. For accurate and representative predictions, a mission profile based on the typical use of the FMTV truck is needed. The mission is separated into driving and silent watch as described below.

DRIVING

The design study is focusing on fuel economy improvement as the FMTV truck carries out a typical mission. This mission is described by a speed profile (driving cycle) that the truck must maintain as it drives over an uneven road profile. The specific road and speed profiles, which consist of city, highway, and cross-country roads, shown in Figure 13, represent a typical mission of the FMTV vehicle. Note that the beginning of the cycle represents the primary and secondary roads with a flat surface and frequent accelerations and decelerations. In the third, cross-country part, driver attempts to maintain constant speed on roads with uneven profile. The driver model adjusts the throttle and brake signal in order for the vehicle to follow the prescribed speed profile. In addition, the engine needs to provide power for the air conditioner and on board electronics according to the duty-cycle described in the next section.

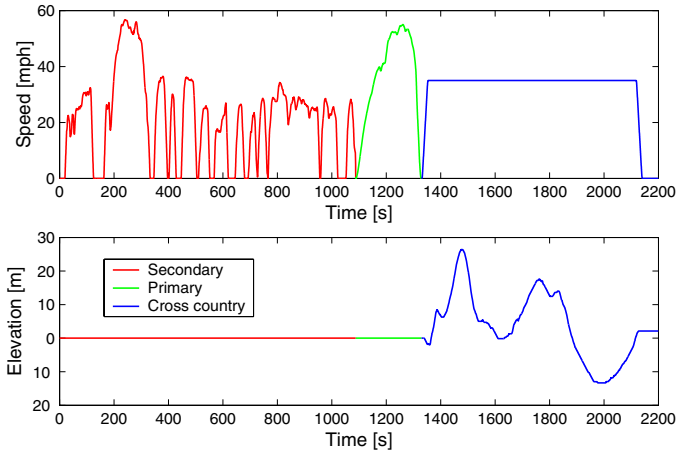

Figure 13: Vehicle driving schedule (50% secondary roads, 20% primary roads, and 30% cross-country)

A power steering model is also included in the mission for more realistic fuel economy predictions. The selected model is very simple with a predefined torque load applied to the engine. The torque varies from a high value when the vehicle steers, to low when it drives straight with no steering. This results in a steering torque pulses when the vehicle steers. The duration of the pulses is set to 2 seconds and the low and high torque values are determined from measurements.

The timing of the pulses (steering event) is defined using a statistical approach. A steering event is initiated based on a steering probability that represents typical driver/vehicle steering behavior as a function of vehicle speed (see Figure 14). At zero speed the steering probability is zero; however, it rapidly increases as the vehicle starts to move, reaching its maximum at a vehicle speed of 7 mph. After that point, the steering probability slowly decreases in order to return to zero at 100 mph (theoretical). The shape of this probability is based on a gamma distribution.

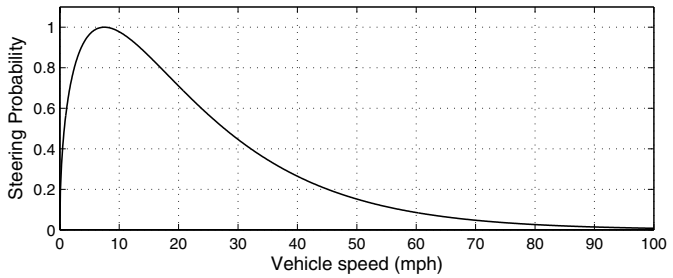

Figure 14: Probability distribution of power steering usage as a function of vehicle speed

The probability distribution is used along with the total usage of steering to generate the steering cycle. The overall steering usage depends on the driving conditions and it can be determined from previous SAE studies/standards [26]. For the driving cycle considered in this study, the steering usage is 60% for secondary roads, 10% for primary roads, and 35% for cross-country. Using this information and the probability distribution for steering the time history of the power steering pump torque is generated as shown in Figure 15. For example, in the case of primary roads we see frequent steering at low speeds due to the high probability, while higher speeds show sporadic usage.

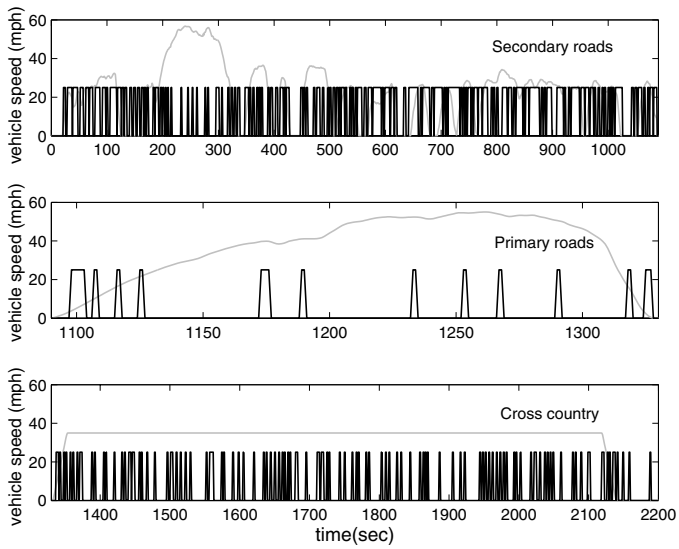

Figure 15: Power steering usage

SILENT WATCH LOADS

The cabin auxiliary loads come from electronics, radio, and ventilation/air conditioning that the driver and soldiers use in the cabin during driving and standby conditions. These loads appear in the form of electric power and are assumed to be the same for both driving and standby conditions, as long as the truck is manned and performing a mission.

More specifically, the electronics load is assumed constant at 0.6 kW since all these devices are turned on throughout the entire time that the vehicle is on a mission. The radio load is assumed to have a peak value of 0.6 kW (zero when not used), and it occurs during 6% of the mission time. The duration of each

interval of usage (pulse) is 40 seconds, which is randomly distributed over time. Finally, the air conditioning is assumed to have a periodic use with 3.4 kW peak power consumption and a period of 8 minutes. In addition, the air conditioning stays on for 2 minutes each time it is turned on, which is representative operation of commercial air conditioning systems. To determine the total power consumption, the power requirements for the three devices are added. This produces the duty cycle shown in Figure 16, with a peak electric load of 4.6 kW and a minimum of 0.6 kW.

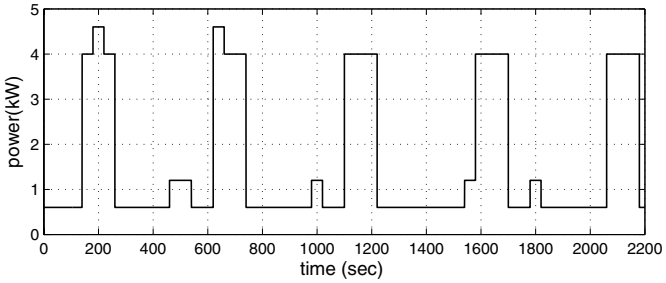

Figure 16: Combined accessory duty cycle during silent watch conditions

SIMULATION RESULTS

The study of the silent watch was performed first. Fuel consumption predictions were obtained for the ten-hour silent watch mission, using the accessory loads and duty cycles described previously. Two vehicle configurations were compared: one relying on the main propulsions diesel engine to generate power, and the other using a 10 kW FC APU. In the baseline vehicle, the 246 kW engine was operated at near-idle conditions to support both electrical and mechanical loads. Summary of results is shown in Table 2. The effect of avoiding inefficient engine operation at near-idle conditions and replacing it with the FC APU is impressive. The fuel consumption decreases from 8.6 gallons to 1.5 gallons with the APU, an 82.6% reduction.

The distribution of visitation points across the FCS load range during 10 hours of silent watch shown in Figure 17 helps explain the benefits. The fuel cell is relatively oversized for silent watch, since it has to accommodate the additional loads during driving. Consequently, the operating points are concentrated in the low current region. Contrary to engines that obtain their peak efficiency at high loads, the fuel cell achieves its best efficiency at very low loads, hence the big impact of replacing engine idling with a FC APU. The FCS average efficiency is 50% and the FP conversion efficiency is 55%, thus the overall FC APU efficiency is 28%. It is clear that reforming of the complex fuel significantly diminishes the overall efficiency to a level attainable with a small diesel powered APU. Nevertheless, the low thermal signature and noise level of the fuel cell APU makes it attractive. The efficiency results rely on the current level of technology and represent a realistic short-term outlook, while expected advances of the fuel cell and reforming technology could significantly improve the long-term perspective.

Table 2: Predicted fuel consumption during the ten hour silent watch for the baseline vehicle, and the one equipped with the Fuel Cell APU.

Energy Source	Fuel consumed [gallon]	Improvement
Diesel engine @ idle speed	8.6	-
Fuel Cell APU	1.5	575%

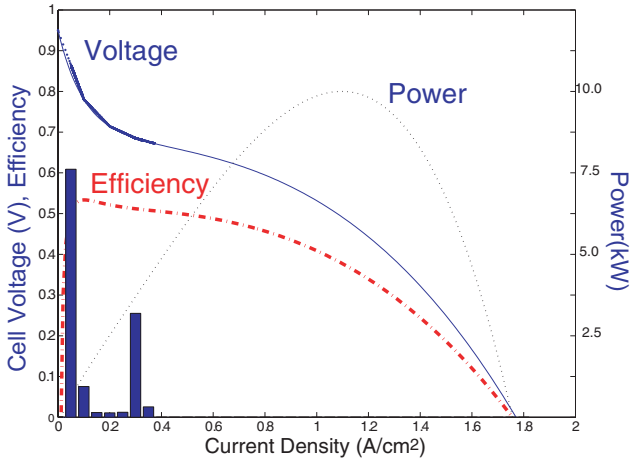

Figure 17: Fuel Cell Stack distribution of visitation points during silent watch

The effect of FC APU during driving was evaluated through simulations over the previously described vehicle duty cycle. Four vehicle system configurations were considered: baseline diesel hydraulic hybrid truck, vehicle with the FC APU added, vehicle with the FC APU and power management strategy allowing engine shut-downs when the vehicle is stopped, and finally the configuration that includes engine downsizing (or de-rating) to 95% of the original power plant. The overall fuel economy results are summarized in Table 3.

The first of the three proposed vehicle designs with the FC APU improves fuel economy over a typical driving schedule by 5.8%. The savings are in part due to the reduction of the diesel propulsion fuel consumption, and in part due to the reduction of fuel consumed for powering accessories. The latter can be attributed to two factors: reduced energy consumption of the controllable, electrified accessories and relatively efficient energy conversion in the APU. Normally the hydraulic hybrid powertrain does not allow engine shut-downs, since engine needs to run the essential accessories at all times. However, electrification of the power steering and air brake compressor allows safe shut-downs, thus increasing the fuel economy benefit to 9.2%. Downsizing the engine by 5% provides only an incremental improvement. Obviously the majority of engine visitation points are in the mid-load range of the engine where small changes of relative load do not have a dramatic impact on specific fuel consumption.

Table 3: Predicted fuel consumption over the FMTV driving schedule and the percent improvement for three configurations of the vehicle equipped with the FC APU.

Energy Source	Propulsion Fuel Cons. [gallon]	Accessory Fuel Cons. [gallon]	Improve-ment
Diesel engine only	2.28	0.369	-
Engine + Fuel Cell APU	2.22	0.306	5.8%
Engine + Fuel Cell APU (Engine shutdown)	2.14	0.306	9.2%
Engine + Fuel Cell APU (Engine shutdown & downsizing to 95%	2.11	0.306	10.6%

Figure 18 shows the engine visitation points as function of speed and load, and illustrates the effect of electrifying accessories and power management strategies on the diesel engine. First of the enlarged sections from right-to-left shows a large number of operating points at low load and idle speed, corresponding to the engine in the baseline vehicle overcoming losses in the torque converter and running the accessories while the vehicle is stopped. The second enlarged section shows changes brought about by electrification of accessories and connecting them to the APU: there are much fewer engine operating points at near idle condition, with a single large spike associated with the engine overcoming the loss in the torque converter during idling. The last insert, far left, indicates further dramatic reduction in the number of near-idle points in case when the engine is being shut-down during extended vehicle stops. Since the very low load engine operation represents the least efficient region, elimination of near-idle points directly and significantly benefits the overall propulsion system efficiency.

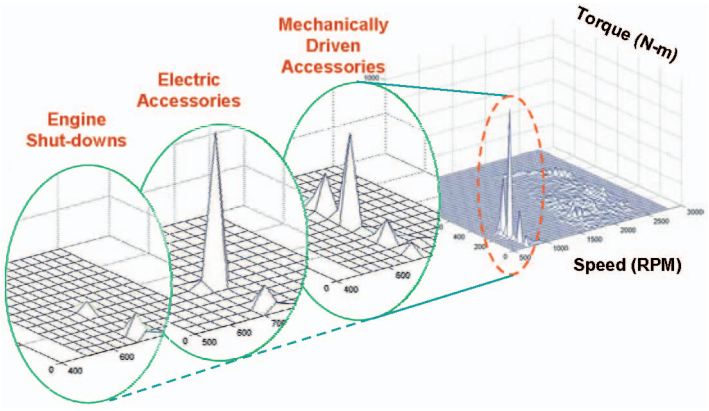

Figure 18: Changes of the distribution of engine visitation points shown as a function of engine speed and load. Magnified portions of the 3-D plot illustrate reduction of near-idle times due to electrification of accessories and engine shut-downs.

The savings realized through the dramatic reduction of the time the engine spends at near-idle conditions are in part offset by the effect of decoupling the accessories from the engine and thus changing the relative position of operating points on the Break Specific Fuel Consumption (BSFC) map. In short, the engine operating point in the baseline system is determined by the sum of the propulsion power and the accessory power. If the accessory power is removed, the relative load of the engine decreases. This means that the point moves downward on the engine BSFC map as shown in Figure 19. If this happens in the low-to-mid speed and part load region, the effect can be relatively significant – see example "A" in Figure 19. However, at higher speeds and loads, the effect might be non-existent – example "B" on Figure 19. In the particular study, the overall effect was not very large, given the very small change between runs with the regular engine and the downsized (95%) engine. However, in case larger accessories are decoupled and connected to the Auxiliary Power Unit, engine downsizing would be highly recommended in order to avoid any offsets of fuel economy gains.

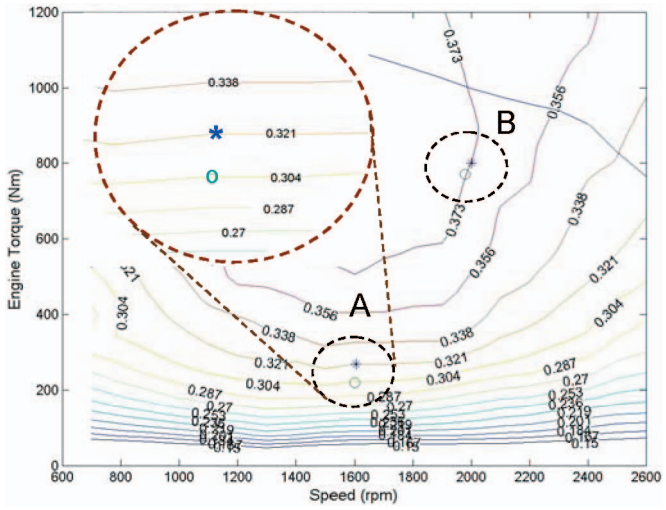

Figure 19: The effect of unloading the engine due to decoupling of the accessories on its efficiency: 'stars' mark operating points with accessories, and 'circles' the corresponding points without accessories.

During driving, the simultaneous operation of cabin accessory devices and engine/drivetrain accessories causes very dynamic APU load changes. Figure 20 shows the instantaneous desired FC APU power (solid), the power delivered by the fuel cell stack (dashed), and the corresponding battery power during a portion of the driving cycle. Whenever the rate of change of load exceeds the ability of the FC system to respond, e.g. when driver suddenly turns the steering wheel, the battery compensates as indicated by the spikes in battery power plot in Figure 20. Note that at the end of the event, e.g. when the steering wheel returns to neutral position, the FC system does not return instantaneously to zero load but slowly ramps down as dictated by the first order lag response. During the power-down events, the FC automatically recharges the battery by using the generated hydrogen from the FP system instead of purging it – see the spikes with the opposite sign in Figure 20. This eliminates the need for a high gain controller for battery recharging.

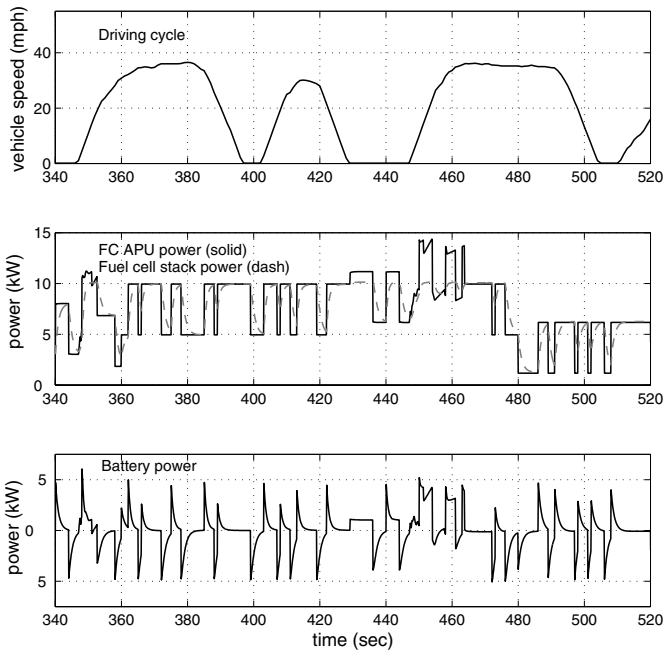

Figure 20: APU and battery response during driving

The distribution of FC visitation points during the driving cycle is shown in Figure 21. In this case, the increased power demand due to the addition of electrified engine/drivetrain accessories moves a number of points towards the high current region, with detrimental effects on average FC efficiency that drops to 47%. The overall FC APU efficiency is as low as 26%.

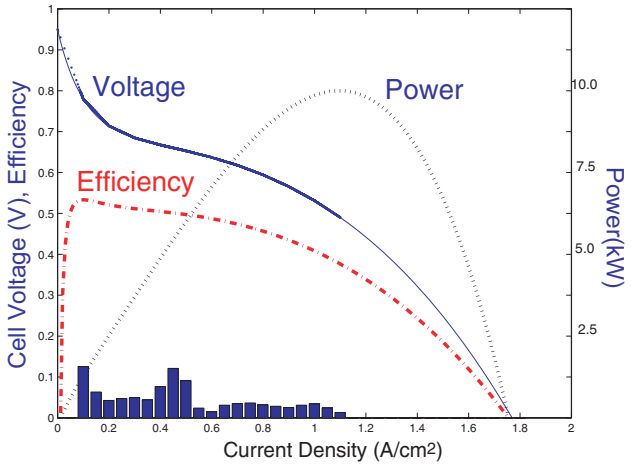

Figure 21: Distribution of FCS visitations points during the FMTV driving schedule

Finally, an attempt is made to assess the realistic impact of the electrification and the use of FC APU from the point of view of the fleet operator and logistics planner. To this end, a hypothetical FMTV truck work day is considered, consisting of 10 hours of driving, 10 hours of silent watch and 4 hours of rest. In this scenario, the daily fuel consumption is reduced from 51.9 to 41.5 gallons, which represents a 20.1% improvement of fuel economy and potential extension of vehicle range by roughly 70 miles.

CONCLUSIONS

The simulation study quantifies the fuel economy benefits of a combined approach of using the Fuel Cell Auxiliary Power Unit (FC APU) for supporting the silent watch requirements, and for powering the selected electrified engine accessories during driving. Models of the low pressure PEM fuel cell stack and the JP8 partial oxidation reformer were derived, accounting for the efficiency of main energy/chemical conversion devices, as well as the effect of fuel choice on overall system efficiency. The virtual vehicle is based on the comprehensive model of the 5-ton, Family of Medium Tactical Vehicles (FMTV) 6x6, Class VI truck with hydraulic hybrid propulsion system, previously modeled in the Automotive Research Center. The silent watch mission defines the use of advanced communication, navigation, computer and Air Conditioning (A/C) and Nuclear Biological and Chemical (NBC) protection systems. The engine/drivetrain accessories decoupled from the engine were the engine oil pump, the air brake compressor and the power steering pump. The peak power requirements of all electrified accessories were estimated at 11.4 kW, out of which 4.6 kW is the peak silent watch power. The fuel cell APU was sized for 10 kW output, assuming that the battery will provide a buffer in case of rare maximum power peaks.

Simulation of the ten-hour silent watch mission indicates the potential for a six-fold improvement of fuel economy compared to the option of idling the diesel engine normally used for propulsion. The results emphasize the fact that the APU eliminates the most inefficient engine operation at very low loads, and replaces it with efficient part load operation of the relatively oversized Fuel Cell system. Fuel savings over the FMTV's combined on-off-road driving schedule were relatively modest at ~6%. The benefits come from operating the controllable electrified components at the optimum conditions, independently of engine speed, and efficient power generation by the FC APU. However, this is somewhat offset by the fact that unloading the accessories from the main-engine moves its operating points to regions of slightly higher specific fuel consumption. Strategically selected engine and drivetrain accessories allow engine shut-downs when the vehicle is stopped, increasing the fuel economy improvement to ~9%.

Compounded fuel economy benefits calculated over the hypothetical daily military mission with a combined highway/local/off-road driving for 10 hours and silent watch for 10 hours, are ~20%. All results were obtained assuming conservative estimates of fuel cell efficiencies attainable in the short term. Reformer efficiency is also low at ~50% due to the fact that it processes a complex fuel (JP8). Fuel choice was dictated by the application of the APU on a military truck. Projected advances in the fuel cell and reformer technology would improve the long term fuel economy potential, and reduce the space and packaging burden.

ACKNOWLEDGMENTS

The authors would like to acknowledge the technical and financial support of the Automotive Research Center (ARC) by the National Automotive Center (NAC) located within the US Army Tank-Automotive Research, Development and Engineering Center (TARDEC). The ARC is a U.S. Army Center of Excellence for Automotive Research at the University of Michigan, currently in partnership with University of Alaska-Fairbanks, Clemson University, University of Iowa, Oakland University, University of Tennessee, Wayne State University, and University of Wisconsin-Madison. In particular, Jim Yakel, Don Szkubiel, Ron Chapp, and Ken Deylami provided technical guidance related to the FMTV Program goals. Herb Dobbs, Erik Kallio (Alternative Fuels & Fuel Cell Team), Jim Miodek and Fred Krestik (Team Power) provided valuable information about hotel loads and battery characteristics. Finally, the authors would like to thank Dave Allen and Bob Page (Engineered Machined Products Inc.) for providing the FMTV engine accessory load data, Bob Julian (Stewart and Stevenson) for air compressor data and John Bennett (Arvin Meritor) for air-brake system data.

REFERENCES

1. Dobbs, H.H, Kallio, E.T., Pechacek, J.M., “U.S. Army Strategy for Utilizing Fuel Cells as Auxiliary Power Units,” SAE paper 2001-01-2792.
2. Lin, C. C., Filipi, Z., Wang Y. S., Louca L., et al, “Integrated, Feed-forward Hybrid Electric Vehicle Simulation in SIMULINK and Its Use for Power Management Studies”, SAE Paper 2001-01-1334, Warrendale, PA, 2001
3. Wu, B., Lin, C., Filipi, Z., Peng, H., Assanis, D., “Optimization of Power Management Strategies for a Hydraulic Hybrid Medium Truck,” 6th International Symposium on Advanced Vehicle Control, Hiroshima, Japan, September 2002
4. Filipi, Z.S., L.S. Louca, B. Daran, Chan-Chiao Lin, U. Yildir, B. Wu, M. Kokkolaras, D.N. Assanis, H. Peng, P.Y. Papalambros, and J.L. Stein, 2003. “Combined Optimization of Design and Power Management of the Hydraulic Hybrid Propulsion System for the 6x6 Medium Truck”; to appear in the Special Issue on Advanced Vehicle Design and Simulation of the International Journal of Heavy Vehicle Systems, Inderscience Publishers, Geneve, 2004
5. Kepner, R.D.,“Hydraulic power assist ~a demonstration of hydraulic hybrid vehicle regenerative braking in a road vehicle application”, SAE paper 2002-01-3128, Warrendale, PA, 2002
6. Venturi, M., Martin, A.,”Liquid-fueled APU fuel cell system for truck application”, SAE paper 2001-01-2716, Warrendale, PA, 2001
7. Venturi, M., Kallio, E., Smith, S., Baker, J., Dhand, P.,“Recent results on liquid-fuelled APU for truck application”, SAE paper 2003-01-0266, Warrendale, PA, 2003
8. Zizelman , J., Botti, J., Tachtler , J., Strobl, W.,“Solid oxide fuel cell auxiliary power unit ~ A paradigm shift in electric supply for transportation”, SAE paper 2000-01-C070, Warrendale, PA, 2000
9. Brodrick, C. J., Farshchi, M., Dwyer, H.A., Gouse, S.W., Martin, J., Von Mayenburg, M.,, “Demonstration of a proton exchange membrane fuel cell as an auxiliary power source for heavy trucks”, SAE paper 2000-01-3488, Warrendale, PA, 2000
10. Hnatczuk, W., Lasecki, M. P., Bishop, J., Goodell, J., “Parasitic loss reduction for 21st century trucks”, SAE paper 2000-01-3423, Warrendale, PA, 2000
11. Hendricks, T., O'Keefe, M., Laboratory “Heavy vehicle auxiliary load electrification for the essential power system program: Benefits, tradeoffs, and remaining challenges”, SAE paper 2002-01-3135, Warrendale, PA, 2002
12. Pukrushpan, J.T., Stefanopoulou, A.G., Varigonda, S., Pedersen, L. and Ghosh, S. “Multivariable Control of Natural Gas Reformer for Fuel Cell Power Plant,” Proceedings of the American Control Conference, 2003
13. Gelfi, S., Pukrushpan, J., Stefanopoulou, A.G., Peng, H. “Dynamics and Control of Low and High Pressure Fuel Cells,” Proceedings of the American Control Conference 2003
14. Brown, L.F. “A Comparative Study of Fuels for On-Board Hydrogen Production for Fuel-Cell-Powered Automobiles,” International Journal of Hydrogen Energy, v.26, pp. 381-397, 2001
15. Pukrushpan, J.T., Peng, H., Stefanopoulou, A.G. “Simulation and Analysis of Transient Fuel Cell System Performance Based on a Dynamic Reactant Flow Model,” Proceedings of the ASME International Mechanical Engineering Congress & Exposition, 2002
16. Ahmed, S., Krumpelt, M. “Hydrogen from Hydrocarbon Fuels for Fuel Cells,” International Journal of Hydrogen Energy, v.26, pp. 291-301, 2001
17. Dicks, A.L., “Hydrogen Generation from Natural Gas for the Fuel Cell Systems of Tomorrow,” Journal of Power Sources, v.61, pp.113-124, 1996
18. Ballard Power System Inc. “Xcellsis HY-80 Light Duty Fuel Cell Engine Brochure,” http://www.ballard.com/pdfs/XCS-HY-80_Trans.pdf, 2003
19. Steele, B., Heinzel, A., “Materials for Fuel Cell Technologies,” Nature, v.414, pp.345 – 352, 2001

20. Louca, L.S., Yildir, U.B.,“Modeling and Reduction Techniques for Studies of Integrated Hybrid Vehicle Systems”. Proceedings of the 4th International Symposium on Mathematical Modeling, Vienna, Austria. Published in the series ARGESIM-Reports, ISBN 3-901608-24-9, Vienna, Austria, 2003.
21. Assanis, D.N., Filipi Z.S., Gravante S., Grohnke D., Gui X.,Louca L.S., Rideout G.D., Stein J.L., Wang Y., “Validation and Use of SIMULINK Integrated, High Fidelity, Engine-In-Vehicle Simulation of the International Class VI Truck”, SAE Paper 2000-01-0288, Warrendale, PA, 2000.
22. Louca, L.S., J.L. Stein, and D.G. Rideout, 2001. “Integrated Proper Vehicle Modeling and Simulation Using a Bond Graph Formulation”. Proceedings of the 2001 International Conference on Bond Graph Modeling, Vol. 33, No. 1, pp. 339-345, Phoenix, AZ. Published by the Society for Computer Simulation, ISBN 1-56555-221-0, San Diego, CA.
23. Karnopp, D.C., D.L. Margolis, and R.C. Rosenberg, “System Dynamics: A Unified Approach”, Wiley-Interscience, ISBN 0471-62171-4, New York, 1990.
24. Brown, F.T., “Engineering System Dynamics: A Unified Graph-Centered Approach”, Marcel Dekker, ISBN 0-8247-0616-1, New York, 2001.
25. Louca, L.S., J.L. Stein, G.M. Hulbert, and J.K. Sprague, “Proper Model Generation: An Energy-Based Methodology”. Proceedings of the 1997 International Conference on Bond Graph Modeling, Vol. 29, No.1, pp. 44-49, Phoenix, AZ. Published by the Society for Computer Simulation, ISBN 1-56555-103-6, San Diego, CA, 1997
26. SAE Standard 1343:” Information Relating to Duty Cycles and Average Power Requirements of Truck and Bus Engine Accessories”